Kinetics and Catalysis, Vol. 46, No. 3, 2005, pp. 396–402. Translated from Kinetika i Kataliz, Vol. 46, No. 3, 2005, pp. 423–429.

ESR Study of the Formation of O_2^- Radical Anions on Oxidized CeO_2 and CeO_2/ZrO_2 Adsorbing a $CO + O_2$ Mixture

A. N. Il'ichev, A. M. Kuli-zade, and V. N. Korchak

Semenov Institute of Chemical Physics, Russian Academy of Sciences, Moscow, 119991 Russia

Received January 26, 2004

Abstract—It is demonstrated by ESR measurements that $O_2^-(CO + O_2)$ radical anions result from $CO + O_2$ adsorption on the oxidized surface of CeO_2. These radical anions are stabilized in the coordination sphere of Ce^{4+} cations located in isolated and associated anionic vacancies. This reaction shows an activation behavior determined by CO adsorption. The variation of $O_2^-(CO + O_2)$ concentration with CO adsorption temperature suggests that surface carbonates and carboxylates participate in this reaction. In the (0.5–10.0)%CeO_2/ZrO_2 system, O_2^- forms on supported CeO_2 and is stabilized on Ce^{4+} and Zr^{4+} cations. The stability of O_2^-–Ce^{4+} complexes is lower on supported CeO_2 than on unsupported CeO_2, indicating a strong interaction between the cerium cations and the support.

INTRODUCTION

Catalytic systems based on CeO_2, ZrO_2, and CeO_2–ZrO_2 are promising for heterogeneous selective catalytic reduction of NO_x (x = 1, 2) with hydrocarbons in excess oxygen and for neutralization of NO_x, CO, and hydrocarbons [1–3]. Although these reactions have been the subject of numerous studies, their mechanism remains disputable [1, 4].

Assuming that NO_x and O_2 can be activated on CeO_2 and ZrO_2, we studied the adsorption of $NO_x + O_2$ mixtures on these oxides and found radical anions O_2^- on their surface. These radical anions do not form during O_2 adsorption in the absence of NO_x [5–7]. Investigation of the mechanism of $O_2^-(NO + O_2)$ formation on CeO_2 and ZrO_2 demonstrated that NO interacts with M^{4+}–O^{2-} (M^{4+} = Zr^{4+}, Ce^{4+}) sites to form M^{4+}–NO_2^{2-} adsorption complexes in which the cation charge then changes from 4+ to 3+ through electron transfer from NO_2^{2-} to M^{4+}. Subsequent interaction between M^{3+} and an O_2 molecule gives O_2^- on the M^{4+} cation [6, 7].

Radical anions O_2^- are known to be intermediates in the low-temperature oxidation of CO on cerium oxide and cerium-containing catalysts [8, 9]. This allowed us to assume that $O_2^-(NO + O_2)$ is involved in CO oxidation upon adsorption of a $CO + NO + O_2$ mixture on CeO_2. To confirm this assumption, we studied the influence of preliminarily adsorbed CO on the formation of $O_2^-(NO + O_2)$ on CeO_2 and found that CO adsorption increases the amount of O_2^- by a factor of ~3. This effect turned out to be due to the formation of O_2^- upon $CO + O_2$ adsorption. Here, we report on this reaction, for it is important for understanding the mechanism of CO oxidation and O_2^- formation upon $NO_x + O_2$ adsorption on CeO_2, ZrO_2, and CeO_2–ZrO_2.

We studied the formation of O_2^- radical anions upon $CO + O_2$ adsorption on oxidized CeO_2 ($O_2^-(CO + O_2)$) at sample oxidation temperatures of 300–700°C, under different adsorption conditions, and for different amounts of CeO_2 supported on ZrO_2. The interaction of O_2^- with molecules NO, NH_3, and CO was also studied.

EXPERIMENTAL

Cerium and zirconium oxides with a specific surface area of S_{sp} = 50 m^2/g were obtained by decomposing $Ce(NO_3)_4 \cdot 6H_2O$ and $ZrO(NO_3)_2$ in air at 500°C for 2 h. The specific surface area was determined by the BET method from low-temperature argon adsorption data.

CeO_2/ZrO_2 samples were prepared by impregnating ZrO_2 with cerium nitrate solutions with different salt concentrations (towards a CeO_2 content of (0.5–10.0) mol %) followed by drying at 100°C and calcination at 350°C in air for 5 h. On the assumption that supported cerium ions are uniformly distributed over the ZrO_2 surface in the (0.5–10.0)%CeO_2/ZrO_2 samples, the ratio of the number of cerium ions to the number of surface zirconium ions is from 0.15 to 3.

The formation of $O_2^-(CO + O_2)$ on oxidized CeO_2 and CeO_2/ZrO_2 was studied by ESR. A 50-mg sample was placed in an ESR tube, pumped to 10^{-4} Pa, heated in vacuum at a preset temperature for 1 h, and oxidized

0023-1584/05/4603-0396 © 2005 MAIK "Nauka/Interperiodica"

in O_2 (P_{O_2} = 10^3 Pa) for 20 min. Next, the sample was cooled to 20°C, pumped, and brought in contact with the gas. The amount of molecules adsorbed on the sample was determined from the variation of the gas pressure in a closed reactor during the adsorption or desorption of preliminarily adsorbed gas using a Pirani gage [10]. After adsorption, ESR spectra of adsorption complexes in the X range were recorded at 20 or –196°C on an EPR-V spectrometer with a Diapazon temperature attachment. The amount of paramagnetic species was determined from twice integrated ESR spectra using $CuSO_4 \cdot 5H_2O$ as the standard. The accuracy of these measurements was 20%.

CO, NO, and O_2 were obtained in a vacuum using standard procedures [11].

RESULTS AND DISCUSSION

1. Formation of O_2^- on CeO_2 upon CO + O_2 Adsorption

After CO or O_2(20°C) is admitted to oxidized CeO_2(400–700°C), no ESR signal is observed. A signal appears after O_2 adsorption (P = 10 Pa) on a sample that was preliminarily exposed to CO (P = 10^3 Pa, t = 1–3 min) and then pumped at 20°C. The ESR signal from the CeO_2(400°C) sample falls in a g-factor range of 2.037–2.009 (Fig. 1, curve *1*). As the CeO_2(500–600°C) oxidation temperature increases, the intensity of the ESR signal increases and a new line appears at g = 2.045 (Fig. 1, curve *2*). For better resolution, the ESR spectrum of CeO_2(600°C) was recorded at –196°C in vacuum (Fig. 1, curve *3*). The g factors derived from spectrum *3* are characteristic of the ESR spectrum of O_2^-, which is detected upon oxygen adsorption on reduced CeO_2 preaged in vacuum at T = 450°C for 1 h or in H_2 at P = 10^3 Pa and T = 400°C for 10 min. According to published data [12], the line with g_1 = 2.029, g_2 = 2.016, and g_3 = 2.011 and the line with g_1 = 2.037 and g_2 = 2.011 in spectrum *3* can be assigned to radical anions O_2^- located in the coordination sphere of Ce^{4+} cations in isolated anionic vacancies. The line with g_1 = 2.052, g_2 = 2.009, and g_3 = 2.006 and the line with g_1 = 2.045, g_2 = 2.011, and g_3 = 2.009 are due to O_2^- radical anions adsorbed on cations in associated anionic vacancies with an increased electron density. It is assumed that O_2^- can be stabilized on Ce^{3+} cations.

Thus, we believe that the adsorption of CO + O_2 on oxidized CeO_2 produces O_2^-(CO + O_2) radical anions stabilized on isolated and associated anionic vacancies. Associated sites are observed on the surface after CeO_2 oxidation in oxygen at T > 400°C.

O_2^-(CO + O_2) radical anions on CeO_2(600°C) are stable at –196°C. Their concentration on the surface in an oxygen medium at 10 Pa and 20°C (5.5×10^{16} m^{-2}) is invariable in time. However, the total concentration of O_2^- located on both isolated and associated Ce^{4+} cations decreases to 2.0×10^{16} m^{-2} as the sample is pumped for 50 min. Readsorption of O_2 or CO + O_2 does not increase the amount of O_2^-. O_2^- radical anions decompose completely upon heating of the sample in vacuum at 100°C for 10 min. CeO_2 regains its activity in the formation of O_2^-(CO + O_2) on being oxidized at $T \geq$ 400°C.

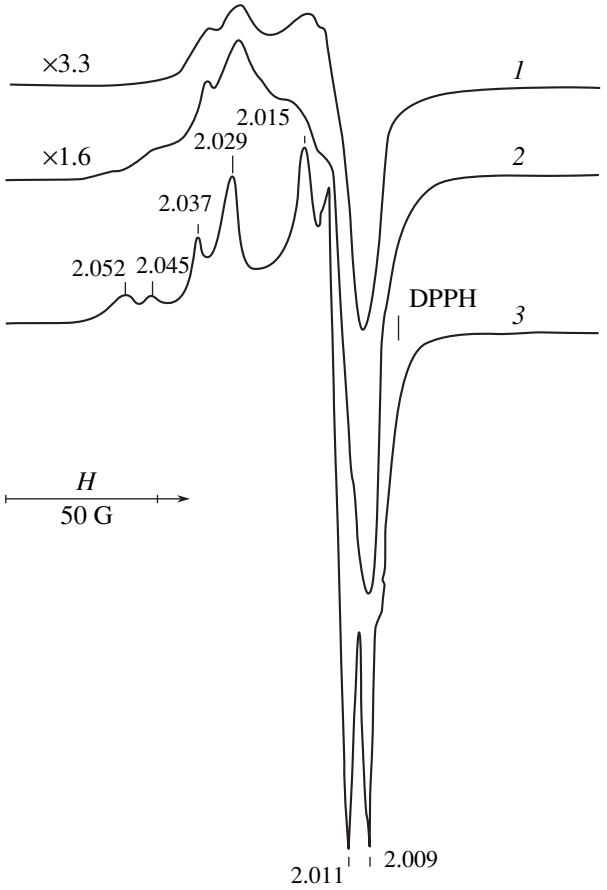

Fig. 1. (*1*, *2*) ESR spectra recorded at 20°C for CeO_2 preaged in O_2 at (*1*) 400 and (*2*) 600°C after CO adsorption (P = 10^3 Pa) for 3 min, pumping, and admission of O_2 (P = 10 Pa) at 20°C. (*3*) Spectrum recorded after sample *2* is cooled to –196°C and pumped.

The amount of O_2^-(CO + O_2) as a function of CeO_2 oxidation temperature was studied as follows. First, CeO_2 was oxidized at a chosen temperature. Next, CO (P = 10^3 Pa) was adsorbed onto the sample over 3 min, the sample was pumped, O_2 (10 Pa) was let in, and the ESR spectrum of O_2^- was recorded at 20°C. Next, the CeO_2 oxidation temperature was increased and O_2^- was formed on the CeO_2 sample under the same CO and O_2 adsorption conditions. The plot of the amount of O_2^-(CO + O_2) versus CeO_2 oxidation temperature is

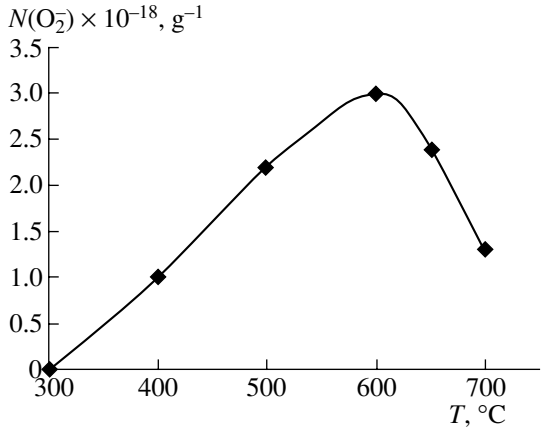

Fig. 2. $O_2^-(CO + O_2)$ concentration as a function of CeO_2 oxidation temperature. For O_2^- formation conditions, see the text.

presented in Fig. 2. As the temperature increases from 300 to 650°C, the amount of O_2^- increases from zero to 3×10^{18} g^{-1}, indicating an increase in the number of active sites involved in O_2^- formation. As the oxidation temperature is further raised to 700°C, this number decreases to 1.5×10^{18} g^{-1}. It does not regain its initial value after the preaging temperature is again lowered to 600°C. This irreversible decrease in the amount of O_2^- is probably caused by a decrease in the surface area of the sample at $T \geq 650$°C [13].

The amount of O_2^- on CeO_2 depends on the pressure of adsorbable gases (CO and O_2). For example, at 20°C, raising the CO pressure from 10 to 5×10^2 Pa at a constant oxygen pressure of 10 Pa increases the concentration of O_2^- radical anions on CeO_2 (600°C) from 1.5×10^{16} to 6.0×10^{16} m^{-2}. A similar increase in O_2^- concentration is observed as the O_2 pressure is increased from 1 to 10 Pa at $P_{CO} = 1 \times 10^3$ Pa.

Table 1. $O_2^-(CO + O_2)$ concentration as a function of CO adsorption temperature for CeO_2 (600°C)

T, °C	$[O_2] \times 10^{-16}$, m^{-2}	$n(CO + O_2)^* \times 10^{-16}$, m^{-2}	$n(CO)^{**} \times 10^{-16}$, m^{-2}
20	5.0	7.1	5.6
100	7.7	11.0	7.0
200	10.0	31.0	16.0

Note: Experimental conditions: $P_{CO} = 10^3$ Pa; $P_{O_2} = 10$ Pa; O_2 adsorption temperature, 20°C.

* Concentration of gas desorbed from the CeO_2 sample at 600°C after the formation of $O_2^-(CO + O_2)$ on the surface.

** Concentration of gas desorbed from the CeO_2 sample at 600°C after CO adsorption in the absence of oxygen.

The amount of $O_2^-(CO + O_2)$ on CeO_2 depends on adsorption temperature. For example, upon successive adsorption of CO and O_2 in amounts of (5×10^{19})–(5×10^{20}) molecule/g at −196°C, O_2^- is not observed on CeO_2(600°C). However, O_2^- radical anions do form when CO is adsorbed onto the sample at 20°C prior to oxygen adsorption at –196°C.

The variation of O_2^- concentration on CeO_2(600°C) as a function of CO adsorption temperature (T_{CO}) between 20 and 200°C was studied as follows. First, CO ($P = 1 \times 10^3$ Pa) was adsorbed onto a preoxidized sample at a chosen temperature T_{CO} for 5 min. After adsorption, the sample was cooled in CO to 20°C and pumped. Next, O_2 ($P = 10$ Pa) was admitted to the sample and the ESR spectrum of O_2^- was recorded. The sample was then pumped and heated in vacuum (without pumping) to 600°C, and the amount of desorbed gas was determined. After desorption, the sample was oxidized in O_2 at 600°C and CO and O_2 adsorption was repeated in a similar way but at another T_{CO}. It can be seen from the data for CeO_2(600°C) in Table 1 that, as T_{CO} increases from 20 to 200°C, the concentration of O_2^- increases from 5×10^{16} to 10×10^{16} m^{-2}, accompanied by an increase in the amount of gas desorbed after $O_2^-(CO + O_2)$ formation ($n(CO + O_2)$) and in the number of desorbed CO molecules. The latter quantity was measured after CO was adsorbed onto CeO_2(600°C) at $P = 10^3$ Pa and $T_{CO} = 20$–200°C for 5 min.

Thus, the formation of $O_2^-(CO + O_2)$ shows an activation behavior determined by the temperature dependence of CO adsorption rather than by O_2^- formation upon O_2 adsorption on CeO_2. The finding that the concentrations of O_2^- and adsorbed CO increase with increasing CO adsorption temperature indicates that CO adsorption complexes formed at 20–200°C are involved in the reaction.

2. Interaction of $O_2^-(CO + O_2)$ with O_2, NO, NH_3, and CO Molecules

Upon admission of oxygen ($P = 10^3$ Pa) into the CeO_2(600°C) sample, the ESR signal of $O_2^-(CO + O_2)$ decreases by a factor of 1.5 and transforms into a singlet line at $\Delta H_{max} = 34$ G. Pumping the sample for 2–3 min recovers the initial shape and intensity of this signal. These reversible changes in the ESR spectrum of O_2^- are evidence of a dipole–dipole interaction between oxygen molecules and the radical anions.

Upon admission of NO ($P = 10$ Pa, $T = 20$°C), the ESR signal of O_2^- disappears completely and is not

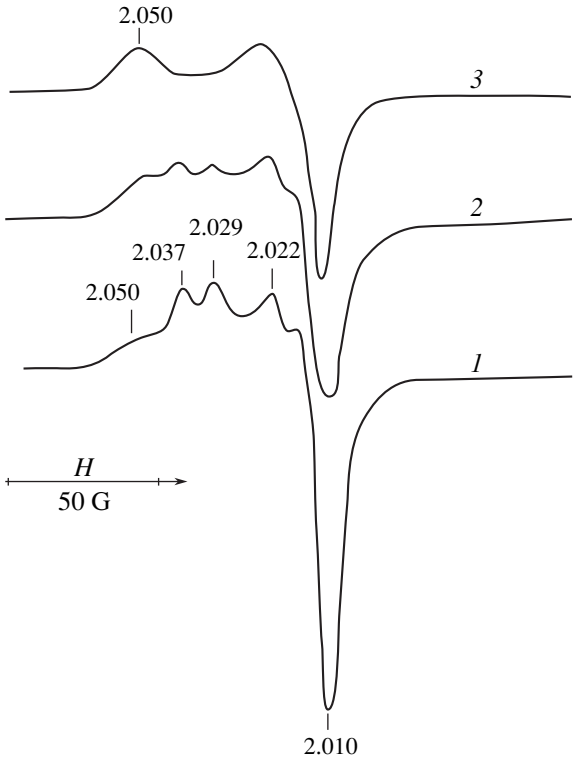

Fig. 3. ESR spectra of O_2^- on CeO_2 at 20°C (*1*) in vacuum and (*2*, *3*) after the adsorption of (*2*) 2×10^{18} and (*3*) 7×10^{18} m^{-2} of NH_3.

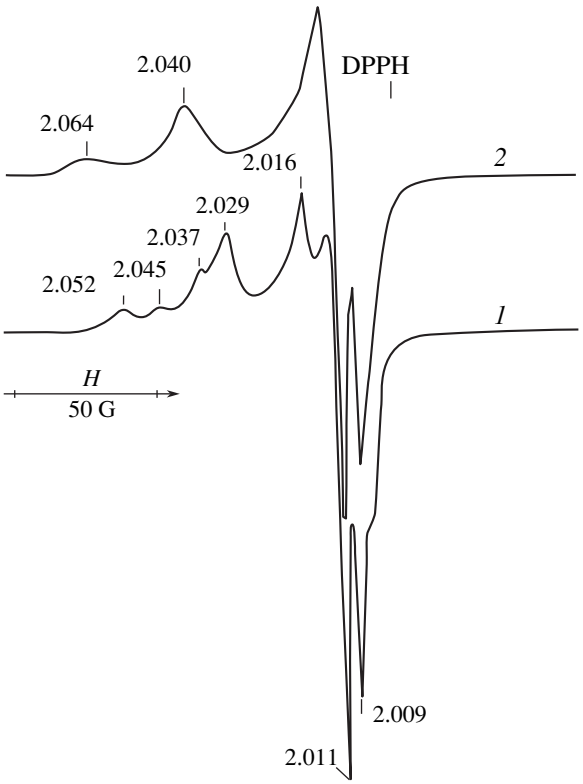

Fig. 4. ESR spectra of O_2^- on CeO_2 at –196°C (*1*) in vacuum and (*2*) after the adsorption of 1×10^{18} m^{-2} CO.

recovered by pumping the sample for 1 h. This is likely to be due to the formation of rather stable nonparamagnetic ($NO–O_2^-$) complexes on the surface.

The interaction of ammonia with O_2^- at 20°C reduces the ESR signal of O_2^- and changes the structure of the spectrum. As can be seen from the data presented in Fig. 3, as the amount of adsorbed NH_3 increases from 2×10^{18} to 7×10^{18} m^{-2}, the intensity of the ESR lines of O_2^- with $g_1 = 2.037$ and 2.029 decreases and the intensity of the line with $g = 2.050$ increases (see curves *2* and *3*). The fact that the intensity of this line increases by a factor of 2 as the total concentration of O_2^- decreases from 6×10^{16} to 3×10^{16} m^{-2} apparently indicates that the lines with $g_1 = 2.037$ and 2.029 shift to higher g factors.

According to the ionic model [14], g_1 increases if ammonia adsorption changes the coordination sphere of the Ce^{4+} cations by weakening the crystal field due to the Ce^{4+} cation on the adsorbed O_2^- radical anion. If this is the case, the distance between the cation and the oxygen radical anion in the $Ce^{4+}–O_2^-$ complex also elongates, which can result in the decomposition of the complexes and in a decrease in the amount of O_2^- on the surface.

Since the authors of several studies assume that O_2^- is involved in CO oxidation, we studied the interaction between CO and O_2^-(CO + O_2) at various temperatures. The ESR spectra of O_2^-(CO + O_2) on a CeO_2(600°C) sample at –196°C in a vacuum (curve *1*) and after CO admission (5×10^{19} g^{-1}) at –196°C (curve *2*) are presented in Fig. 4. Comparing spectra *1* and *2* shows that the interaction between O_2^- and adsorbed CO results in a shift of the ESR line of O_2^- with $g_1 = 2.052–2.029$ to 2.064–2.040. The numbers of spins determined from spectra *1* and *2* are almost the same. Heating this sample to –150°C causes desorption of all the CO, and spectrum *2* transforms into spectrum *1*.

The increase in g_1 in the ESR spectrum of O_2^- upon physical adsorption of CO can be due to the effect of adsorbed CO molecules on the coordination sphere of the cation in the $Ce^{4+}–O_2^-$ complexes, as in the case of the interaction between NH_3 and $Ce^{4+}–O_2^-$.

Upon admission of CO ($P_{CO} = 10^3$ Pa) at 20°C, the ESR spectrum of O_2^- disappears within 1 min. The

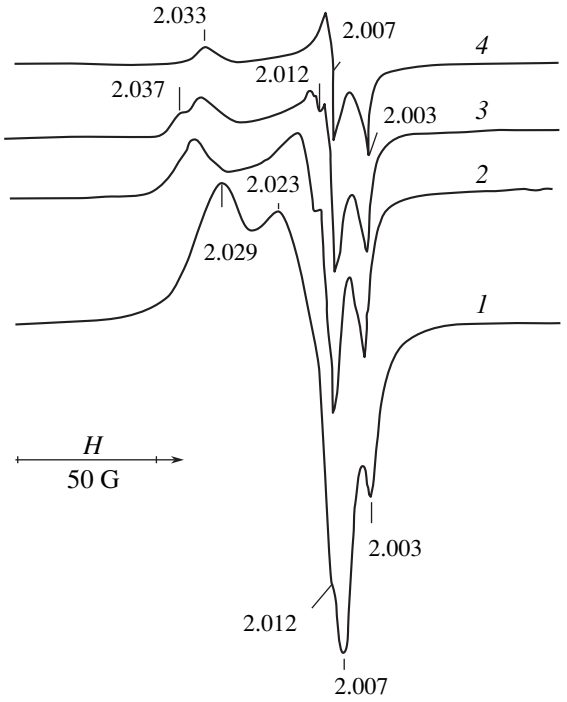

Fig. 5. ESR spectrum of 10%CeO_2/ZrO_2(600°C) (*1*) after CO adsorption ($P = 10^3$ Pa) for 3 min, pumping, and admission of O_2 (P = 10 Pa) at 20°C. (*2–4*) The same spectrum recorded after pumping of O_2 for (*2*, *3*) 3 min at (*2*) 20 and (*3*) 50°C and (*4*) 10 min at 100°C.

spectrum is not recovered by pumping the sample and appears only after admission of oxygen (10–10^2 Pa) but with a lower intensity as compared to the initial spectrum. Thrice repeated treatment of the sample with CO and then O_2 reduces the concentration of O_2^- radical anions from 6×10^{16} to 2×10^{16} m^{-2}, indicating a decrease in the reactivity of CeO_2 under these conditions. The reactivity is completely recovered after 10-min oxidation of CeO_2 in O_2 at 400–600°C.

Table 2. $O_2^-(CO + O_2)$ concentration ($\times 10^{-16}$ m^{-2}) as a function of the CeO_2 content of CeO_2/ZrO_2(500°C) after adsorption of CO ($P = 10^3$ Pa) and O_2 (P = 10 Pa) at 20°C

CeO_2 content of the sample, %	Total concentration of O_2^-	O_2^- concentration on Ce^{4+}
0	0	–
0.5	0.02	–
2.0	0.30	0.15
5.0	1.40	0.80
10.0	2.0	1.60
100	5.0	5.0

Since the rate of O_2^- decomposition at 20°C in vacuum is much lower than the rate of O_2^- conversion in a CO atmosphere, we can assume that CO displaces O_2^- from the coordination sphere of the cation or reacts with it to form CO_2 [8, 9]. The latter assumption is more plausible because the O_2^- concentration remains unchanged after Ar (5×10^2 Pa) is admitted to the sample.

In the oxidation of CO to CO_2 with O_2^- radical anions, the CeO_2 surface is reduced and its interaction with oxygen yields O_2^-. The decrease in O_2^- concentration resulting from several cycles of CO oxidation with O_2^- radical anions is likely to be due to CO_2 molecules blocking the active sites responsible for $O_2^-(CO + O_2)$ formation. These active sites are regenerated at $T \geq$ 400°C.

3. Formation of $O_2^-(CO + O_2)$ on (0.5–10.0)%CeO_2/ZrO_2

As in the case of CeO_2, the adsorption of CO or O_2 (20°C) on oxidized (0.5–10.0)%CeO_2/ZrO_2(500°C) produces no ESR signal. A signal appears upon oxygen adsorption (P = 10 Pa) on specimens with preliminarily adsorbed CO ($P = 10^3$ Pa, t = 3 min). Figure 5 (curve *1*) shows this signal for 10.0%CeO_2/ZrO_2. As this sample is pumped for 2–3 min, the lines with g = 2.028 and 2.023 disappear and the intensity of the line with g = 2.012 decreases (curve *2*). Admission of oxygen recovers these lines. The intensity of these lines depends on oxygen pressure, and their g values are close to the g values for O_2^- on CeO_2 ($g_1 = 2.028$, $g_2 = 2.016$, and $g_3 = 2.011$); therefore, they can be assigned to O_2^- radical anions located on supported Ce^{4+} cations. The finding that this type of O_2^- radical anion is less stable than the O_2^- radical anion on CeO_2 indicates a strong interaction between the ZrO_2 support and the Ce^{4+} cations [15].

Spectrum *2* in Fig. 5 is complicated and consists of two ESR signals. The first is characterized by g values of 2.037 and 2.012. It disappears upon heating of the sample in vacuum at 100°C (curves *3*, *4*). Therefore, it is due to O_2^- radical anions in the coordination sphere of Ce^{4+}. The second signal, characterized by $g_1 = 2.033$, $g_2 = 2.007$, and $g_3 = 2.003$, disappears only after heating of the sample at 270°C for 10 min and is attributed to O_2^- radical anions stabilized on Zr^{4+} cations [6, 7].

The data presented in Table 2 demonstrate how the total concentration of O_2^- depends on the CeO_2 content of CeO_2/ZrO_2(500°C) obtained by adsorption of CO ($P = 10^3$ Pa, t = 3 min) and O_2 (P = 10 Pa) at 20°C. $O_2^-(CO + O_2)$ does not form on pure ZrO_2(500°C). For

(0.5–10.0)%CeO_2/ZrO_2, both the total O_2^- concentration and the concentration of weakly bound O_2^- adsorption species increase with increasing amount of supported CeO_2. The finding that the concentration of weakly bound O_2^- species increases as the cerium content of a supported sample is increased confirms the assumption that these species are stabilized on Ce^{4+} cations.

Thus, $O_2^-(CO + O_2)$ formation on (0.5–10.0)% CeO_2/ZrO_2 occurs only on supported CeO_2 and O_2^- is stabilized on Ce^{4+} and Zr^{4+} cations. O_2^- radical anions can be stabilized on Zr^{4+} cations when the reaction occurs at the oxide interface or when there is spillover of O_2^- from the CeO_2 phase to the ZrO_2 support.

Note that, for (0.5–10.0)%CeO_2/ZrO_2, no O_2^- radical anions were observed on cerium cations located in associated anionic vacancies. Apparently, they do not form because the cerium phase on the ZrO_2 surface is finely dispersed even when the concentration of supported Ce^{4+} ions is three times higher than the concentration of surface Zr^{4+} ions, as in the case of 10.0%CeO_2/ZrO_2.

4. Mechanism of Formation of $O_2^-(CO + O_2)$ on CeO_2

The activation behavior of $O_2^-(CO + O_2)$ formation on CeO_2 is determined by the temperature dependence of the CO adsorption. This is indicated by the fact that both the $O_2^-(CO + O_2)$ concentration and the CO coverage of the surface increase as the CO adsorption temperature increases from 20 to 200°C (Table 1). On the other hand, it is known [16] that CO is oxidized on CeO_2 at $T \geq 400$°C. Therefore, CO adsorption between 20 and 200°C produces surface complexes that are active in the formation of $O_2^-(CO + O_2)$.

According to IR spectroscopic data [17], CO adsorption on the oxidized CeO_2 surface at 20°C results in the formation of a linear CO adsorption species, bidentate and monodentate carbonates, and inorganic carboxylates. The linear CO adsorption species is easily removed by pumping. Therefore, it is not involved in the formation of $O_2^-(CO + O_2)$. The carbonates and carboxylates remain on the surface, and their amount increases as the CO adsorption temperature is increased from 20 to 200°C. The complexes decompose completely at $T \geq 400$°C. This temperature dependence of the formation and decomposition of carbonates and carboxylates correlates well with the way the $O_2^-(CO + O_2)$ concentration on CeO_2 varies with increasing CO adsorption temperature (Table 1) and the fact that CeO_2 regains its activity in $O_2^-(CO + O_2)$ formation upon preaging of the sample at $T \geq 400$°C. Therefore, we can assume that the free electrons involved in $O_2^-(CO + O_2)$ formation are produced during the formation of carbonate or carboxylate complexes.

Evidently, the carbonate and carboxylate complexes result from the oxidation of CO with surface oxygen since this process is retarded on reduced CeO_2 [17]. Furthermore, this process must be accompanied by the reduction of Ce^{4+} cations to Ce^{3+} [18]. Subsequent interaction between the reduced cations and adsorbed O_2 molecules through electron transfer from Ce^{3+} to $O_{2,\,ads}$ affords oxygen radical anions, which are stabilized in the coordination sphere of coordinately unsaturated Ce^{4+} ions.

The coordinately unsaturated Ce^{4+} ions and surface oxygen involved in the formation of $O_2^-(CO + O_2)$ result from the dehydroxylation of CeO_2 as the sample is heat-treated in oxygen. The amount of these species increases with an increase in CeO_2 preaging temperature. This is indicated by increasing $O_2^-(CO + O_2)$ concentration with an increase in CeO_2 oxidation temperature (Fig. 2).

The concentration of coordinately unsaturated Ce^{4+} ions on the oxidized CeO_2(600°C) surface is 7×10^{17} m^{-2} [6]. This value is ten times higher than the observed concentration of $O_2^-(CO + O_2)$. This difference probably arises from the difference between the concentration of O_2^- stabilization centers and the concentration of surface oxygen involved in the formation of electron donors in CO adsorption.

Oxygen species on the CeO_2 surface were considered in earlier works [16, 17]. These include monooxygen ions octahedrally coordinated to cations, bridging dioxygen adsorption species, and O_2^- radical anions. As is demonstrated above, O_2^- radical anions are involved in CO oxidation on CeO_2 at 20°C. It is most likely that this reaction proceeds through the formation of carbonates decomposing at $T \geq 400$°C [17]. We did not observe O_2^- radical anions in the formation of $O_2^-(CO + O_2)$ on the original oxidized CeO_2(400–700°C) specimens. Therefore, the formation of carbonate and carboxylate complexes active in this reaction involves monooxygen ions or bridging dioxygen species.

REFERENCES

1. Daturi, M., Bion, N., Saussey, J., Lavalley, J.-C., Hedouin, C., Seguelong, T., and Blanchard, G., *Phys. Chem. Chem. Phys.*, 2001, vol. 3, p. 252.
2. Bera, P., Patil, K.C., and Hegde, M.C., *Phys. Chem. Chem. Phys.*, 2000, vol. 2, p. 3715.
3. Rodriguez, J., Hanson, J.C., Kim, J.K., and Liu, G., *J. Phys. Chem. B*, 2003, vol. 107, p. 3535.

4. Sadykov, V.A., Lunin, V.V., Matyshak, V.A., Paukshtis, E.A., Rozovskii, A.Ya., Bulgakov, N.N., and Ross, D., *Kinet. Katal.*, 2003, vol. 44, no. 3, p. 412.
5. Konin, G.A., Il'ichev, A.N., Matyshak, V.A., and Korchak, V.N., *Mendeleev Commun.*, 2000, no. 5, p. 197.
6. Il'ichev, A.N., Konin, G.A., and Matyshak, V.A., Kulizade, A.M., Korchak, V.N., and Yan, Yu.B., *Kinet. Katal.*, 2002, vol. 43, no. 2, p. 235.
7. Il'ichev, A.N., Shibanova, M.D., Ukharskii, A.A., Kulizade, A.M., and Korchak, V.N., *Kinet. Katal.*, 2005, vol. 46, no. 3, p. 414.
8. Shubin, V.E., Shvets, V.A., Savel'eva, V.A., Popova, N.M., and Kazanskii, V.B., *Kinet. Katal.*, 1982, vol. 23, no. 5, p. 1153.
9. Sass, A.S., Shvets, V.A., Savel'eva, G.A., Popova, N.M., and Kazanskii, V.B., *Kinet. Katal.*, 1985, vol. 26, no. 4, p. 924.
10. Tret'yakov, I.I., Shub, B.R., and Sklyarov, A.V., *Zh. Fiz. Khim.*, 1970, vol. 44, p. 2112.
11. *Handbuch der preparativen anorganischen Chemie*, von Brauer, G., Ed., Stuttgart: Ferdinand Enke, 1981.
12. Soria, J., Martinez-Arias, A., and Conesa, J.C., *J. Chem. Soc., Faraday Trans.*, 1995, vol. 91, no. 11, p. 1669.
13. Fornasiero, P., Balducci, G., Di Monte, R., Kaspar, J., Sergo, V., Gubitosa, G., Ferrero, A., and Grazini, M., *J. Catal.*, 1996, vol. 164, p. 173.
14. Che, M. and Tench, A.J., *Adv. Catal.*, 1983, vol. 32, p. 1.
15. Soria, J., Coronado, J.M., and Conesa, J., *J. Chem. Soc., Faraday Trans.*, 1996, vol. 92, no. 9, p. 1619.
16. Yao, H.C. and Yao, Y.F., *J. Catal.*, 1984, vol. 86, p. 254.
17. Li, C., Sakata, Y., Domon, T.K., Maruya, K., and Onishi, T., *J. Chem. Soc., Faraday Trans.*, 1989, vol. 4, no. 4, p. 929.
18. Breysse, V., Guenin, M., Cloudel, B., and Veron, J., *J. Catal.*, 1973, vol. 28, p. 54.